

NEW FILTERING TECHNIQUE FOR THE IMPULSIVE NOISE REDUCTION IN COLOR IMAGES

B. SMOLKA, A. CHYDZINSKI, K. N. PLATANIOTIS,
AND A. N. VENETSANOPOULOS

Received 31 October 2001

We present a novel approach to the problem of impulsive noise reduction for color images. The new image-filtering technique is based on the maximization of the similarities between pixels in the filtering window. The method is able to remove the noise component, while adapting itself to the local image structure. In this way, the proposed algorithm eliminates impulsive noise while preserving edges and fine image details. Since the algorithm can be considered as a modification of the vector median filter driven by fuzzy membership functions, it is fast, computationally efficient, and easy to implement. Experimental results indicate that the new method is superior, in terms of performance, to algorithms commonly used for impulsive noise reduction.

1. Standard color noise reduction filters

A number of nonlinear, multichannel filters, which utilize correlation among multivariate vectors using various distance measures, have been proposed to date, [4, 5, 6, 7, 8, 9, 10, 11]. The most popular nonlinear, multichannel filters are based on the ordering of vectors in a predefined moving window. The output of these filters is defined as the lowest ranked vector according to a specific vector-ordering technique.

Let $\mathbf{F}(x)$ represent a multichannel image and let W be a window of finite size n (filter length). The noisy image vectors inside the filtering window W are denoted by \mathbf{F}_j , $j = 0, 1, \dots, n-1$. If the distance between two vectors \mathbf{F}_i , \mathbf{F}_j is denoted by $\rho\{\mathbf{F}_i, \mathbf{F}_j\}$, then the scalar quantity $R_i = \sum_{j=0}^{n-1} \rho\{\mathbf{F}_i, \mathbf{F}_j\}$ is the total distance associated with the noisy vector \mathbf{F}_i .

The ordering of the R_i 's: $R_{(0)} \leq R_{(1)} \leq \dots \leq R_{(n-1)}$, implies the same ordering of the corresponding vectors \mathbf{F}_i : $\mathbf{F}_{(0)} \leq \mathbf{F}_{(1)} \leq \dots \leq \mathbf{F}_{(n-1)}$. Nonlinear ranked-type multichannel estimators define the vector $\mathbf{F}_{(0)}$ as the filter output. However, the concept of input ordering, initially applied to scalar quantities, is not easily extended to multichannel data since there is no universal way to define ordering in vector spaces.

To overcome this problem, distance functions are often utilized to order vectors. As an example, the *vector median filter* (VMF) uses the L_1 , L_2 norms to order vectors according to their relative magnitude differences, [1, 7, 8].

The orientation difference between two vectors can also be used as their distance measure. This so-called *vector angle criterion* is used by the *vector directional filters* (VDF) to remove vectors with atypical directions, [3, 14].

The *basic vector directional filter* (BVDF) is a ranked-order, nonlinear filter which parallelizes the VMF operation. However, a distance criterion, different from the L_1 , L_2 norms used in VMF, is utilized to rank the input vectors. The output of the BVDF is that vector from the input set, which minimizes the sum of the angles with the other vectors. In other words, the BVDF chooses the vector most centrally located without considering the magnitudes of the input vectors.

To improve the efficiency of the directional filters, another method called *directional distance filter* (DDF) was proposed, [3]. This filter retains the structure of the BVDF but utilizes a generalized distance criterion to order the vectors inside the processing window.

Another efficient rank-ordered technique called *hybrid directional filter* (HDF) was presented in [2]. This filter operates in the direction and magnitude of the color vectors independently and then combines them to produce a unique final output.

All standard filters detect and replace well noisy pixels, but their property of preserving pixels which were not corrupted by the noise process is far from ideal. In this paper, we show the construction of a simple, efficient, and fast filter which removes noisy pixels, but has the ability of preserving original image-pixel values.

2. New filtering technique

We start from a gray scale image in order to better explain how the new algorithm is constructed. Let the gray scale image be represented by a matrix F of size $N_1 \times N_2$, $F = \{F(i, j) \in \{0, \dots, 255\}, i = 1, 2, \dots, N_1, j = 1, 2, \dots, N_2\}$.

Our construction starts with the introduction of the similarity function $\mu : [0; \infty) \rightarrow \mathbb{R}$. We will need the following assumptions for μ :

- (1) μ is decreasing in $[0; \infty)$,
- (2) μ is convex in $[0; \infty)$,
- (3) $\mu(0) = 1, \mu(\infty) = 0$.

In the construction of our filter, the central pixel in the window W is replaced by that one, which maximizes the sum of similarities between all its neighbors. Our basic assumption is that a new pixel must be taken from the window W (introducing pixels which do not occur in the image is prohibited like in the VMF and BVDF).

For this purpose, μ must be convex, which can be easily shown. For the gray scale images, we define the following fuzzy measure of similarity between two pixels F_k and F_l (see [12, 13]):

$$\mu\{F_k, F_l\} = \mu(|F_k - F_l|). \quad (2.1)$$

We now assume that F_0 is the center pixel in the window W and the pixels F_1, F_2, \dots, F_{n-1}

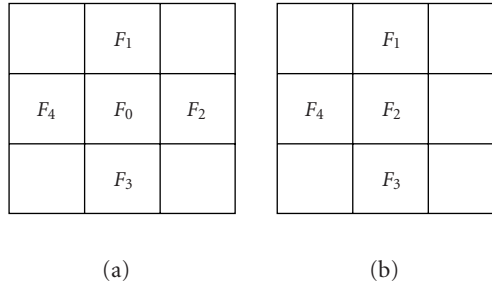


Figure 2.1. Illustration of the construction of the new filtering technique for the 4-neighborhood case. If the center pixel F_0 is replaced by its neighbor F_2 , then the similarity measure $M_2 = \mu\{F_2, F_1\} + \mu\{F_2, F_3\} + \mu\{F_2, F_4\}$ between F_2 (new center pixel) and its neighbors in W is calculated. If the total similarity M_2 is greater than $M_0 = \mu\{F_0, F_1\} + \mu\{F_0, F_2\} + \mu\{F_0, F_3\} + \mu\{F_0, F_4\}$, then the center pixel is replaced, otherwise it is retained.

are surrounding F_0 (Figure 2.1). In the first step of the algorithm, the total sum M_0 of the similarities between the central pixel F_0 , which is suspected to be noisy, and its neighbors F_i , $i = 1, \dots, n-1$, is calculated. In the second step, each of the neighbors of the central pixel is moved to the center of the filtering window and the central pixel F_0 is rejected from W . For each pixel F_i of the neighborhood, which is being placed in the center of W , the total sum of similarities M_i is calculated and then compared with M_0 . It has to be stressed that in the second step the total sum of similarities is calculated without taking into account the original central pixel F_0 , which is rejected from the filter window.

In this way, the central pixel F_0 is replaced by that F_i from the neighborhood, for which the total similarity function M_i , which is a sum of all values of similarities between the central pixel and its neighbors, reaches its maximum. In other words, if

$$M_i = \sum_{j=1}^{n-1} (1 - \delta_{i,j}) \mu\{F_i, F_j\}, \quad i = 1, 2, \dots, n-1, \quad (2.2)$$

where $\delta_{i,j}$ is defined as

$$\delta_{i,j} = \begin{cases} 1 & \text{if } i = j, \\ 0 & \text{if } i \neq j, \end{cases} \quad (2.3)$$

is larger than

$$M_0 = \sum_{j=1}^{n-1} \mu\{F_0, F_j\}, \quad (2.4)$$

then the center pixel is replaced by F_i . Generally, the pixel F_0 is given by the value F_{i_*} , where $i_* = \arg \max_i M_i$,

$$M_i = \delta_{i,0} \sum_{j=1}^{n-1} \mu\{F_i, F_j\} + (1 - \delta_{i,0}) \sum_{j=1}^{n-1} (1 - \delta_{i,j}) \mu\{F_i, F_j\}. \quad (2.5)$$

This approach can be easily extended to color images. In this case, we use the similarity function defined by $\mu\{\mathbf{F}_k, \mathbf{F}_l\} = \mu(\|\mathbf{F}_k - \mathbf{F}_l\|)$, where $\|\cdot\|$ denotes the specific vector norm. Now, in exactly the same way, we can maximize the total similarity function M for the vector case.

In finding the maximum in (2.5), we obtain $(n - 1)$ nonzero components in M_0 . If we replace the central pixel by one of its neighborhoods (by F_2 in Figure 2.1(a)), then we obtain only $(n - 2)$ nonzero components in M , as the pixel which has been put into the center disappears from the filter window (Figure 2.1(b)). In this way the filter tends to replace the original pixel only when it is really noisy and preserves in this way the image structures.

The BASIC code which can be used for the fast computer implementation is presented in Algorithm 2.1.

3. Results

The performance of the new algorithm was compared with the standard procedures of noise reduction used in color image processing.

The color image Lena has been contaminated by impulsive *salt and pepper* noise (pixel channel values are randomly replaced by 0 or 255 with equal probability), and the root of the mean square error (RMSE), peak signal-to-noise ratio (PSNR), and normalized mean square error (NMSE) have been used as quantitative measures of quality for evaluation purposes:

$$\begin{aligned} \text{MSE} &= \frac{\sum_{i=1}^{N_1} \sum_{j=1}^{N_2} \|\mathbf{F}(i, j) - \hat{\mathbf{F}}(i, j)\|^2}{3 \cdot N_1 \cdot N_2}, \\ \text{RMSE} &= \sqrt{\text{MSE}}, \quad \text{PSNR} = 20 \log \left\{ \frac{255}{\text{RMSE}} \right\}, \\ \text{NMSE} &= \frac{\sum_{i=1}^{N_1} \sum_{j=1}^{N_2} \|\mathbf{F}(i, j) - \hat{\mathbf{F}}(i, j)\|^2}{\sum_{i=1}^{N_1} \sum_{j=1}^{N_2} \|\mathbf{F}(i, j)\|^2}, \end{aligned} \quad (3.1)$$

where N_1, N_2 are the image dimensions and $\mathbf{F}(i, j)$ and $\hat{\mathbf{F}}(i, j)$ denote the original pixel vector and the restored vector, respectively.

BASIC CODE OF THE NEW ALGORITHM

$cr(N_1, N_2)$, $cg(N_1, N_2)$, $cb(N_1, N_2)$ - input color image,
 $wr(N_1, N_2)$, $wg(N_1, N_2)$, $wb(N_1, N_2)$ - output color image
 β - similarity function coefficient
 sim - total similarity between pixels in 3×3 window

```

For i=0 To 255
For j=0 To 255
expo(i,j)=Exp(-beta*Abs(i-j))
Next
Next

```

```

For i=2 To N1-1
For j=2 To N2-1
max=-1
For g=-1 To 1
For h=-1 To 1
w=i+g
z=j+h
sim=0
For r=-1 To 1
For s=-1 To 1
x=i+r
y=j+s
If Not w=x Or Not z=y Then
If Not r=0 Or Not s=0 Then
simr=expo(cr(x,y),cr(w,z))
simg=expo(cg(x,y),cg(w,z))
simb=expo(cb(x,y),cb(w,z))
sim=sim+simr+simg+simb
End If
End If
Next
Next
If sim>max Then
max=sim
pixr=cr(w,z)
pixg=cg(w,z)
pixb=cb(w,z)
End If
Next
Next
wr(i,j)=pixr
wg(i,j)=pixg
wb(i,j)=pixb
Next
Next

```

TABLE 3.1 Compared filters.

Notation	Filter	Reference
AMF	Arithmetic mean filter	[1]
VMF	Vector median filter	[6]
ANNF	Adaptive nearest neighbor filter	[10]
BVDF	Basic vector directional filter	[8]
HDF	Hybrid directional filter	[7]
AHDF	Adaptive hybrid directional filter	[7]
DDF	Directional distance filter	[4]
FVDF	Fuzzy vector directional filter	[9]

We investigated the behavior of the proposed filter using various convex functions. The new filter is then compared, in terms of performance, with various filters listed in Table 3.1. The following set of membership functions is considered in this work (Figure 3.1):

$$\begin{aligned}
\mu_1(x) &= e^{-\beta_1 x}, & \beta_1 &\in (0; \infty), \\
\mu_2(x) &= \frac{1}{1 + \beta_2 x}, & \beta_2 &\in (0; \infty), \\
\mu_3(x) &= \frac{1}{(1+x)^{\beta_3}}, & \beta_3 &\in (0; \infty), \\
\mu_4(x) &= 1 - \frac{2}{\pi} \arctan(\beta_4 x), & \beta_4 &\in (0; \infty), \\
\mu_5(x) &= \frac{2}{1 + e^{\beta_5 x}}, & \beta_5 &\in (0; \infty), \\
\mu_6(x) &= \frac{1}{1 + x^{\beta_6}}, & \beta_6 &\in (0; 1), \\
\mu_7(x) &= \begin{cases} 1 - \beta_7 x & \text{if } x < \frac{1}{\beta_7}, \\ 0 & \text{if } x \geq \frac{1}{\beta_7}, \end{cases} & \beta_7 &\in (0; \infty).
\end{aligned} \tag{3.2}$$

Experimental analysis revealed that all these similarity functions can be used effectively in the new filtering structure. Table 3.2 summarizes the values of the parameter β_i used in the various functions μ_i when a test image Lena distorted by impulsive *salt and pepper* noise up to 10% is considered.

Table 3.3 summarizes the results obtained for the test image Lena distorted by 4% impulsive noise. In order to obtain the results reported in Table 3.3, the L_2 norm was used to calculate the differences between the color vectors while the parameter β_i values are those reported in Table 3.2. All proposed functions μ give very good results, although the best results are those obtained using the μ_1 , μ_5 , and μ_7 functions. In a second set of experiments, we tested the effect of the distance measure (norm) on the performance of the new

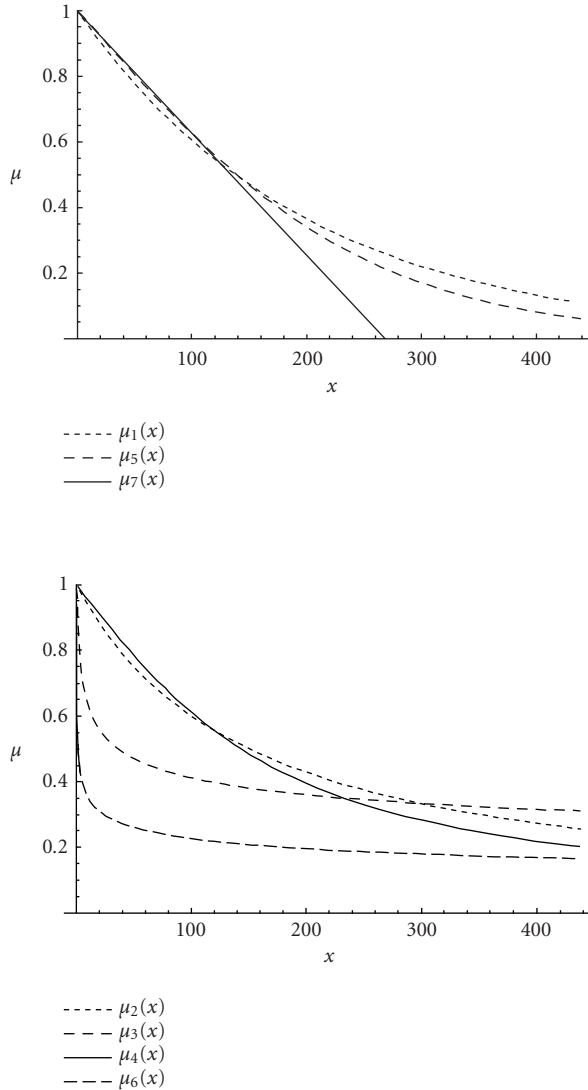


FIGURE 3.1 Plots of the similarity functions $\mu_1(x), \dots, \mu_7(x)$.

filtering algorithm. In these second experiments, only three filters implemented using the “best” similarity functions, namely μ_1 , μ_5 , and μ_7 , are considered. Resulting RMSE values presented in Table 3.4 reveal that the best performance is obtained, as expected, when the Euclidean distance (L_2 norm) is used.

The efficiency of the new filtering technique is shown in Figures 3.2, 3.3, and 3.4. Figure 3.2 depicts the result of noise reduction using the new method applied to a gray scale image Lena in comparison with the standard median filter. The test image was contaminated by 4% salt and pepper noise and a 3×3 filtering mask was used. Figure 3.3

TABLE 3.2 Optimal values of constants β_i [10^{-3}].

β_1	β_2	β_3	β_4	β_5	β_6	β_7
5.04	6.62	192	6.97	7.90	266	3.72

TABLE 3.3 Comparison of the new filter with the standard techniques from Table 3.1. For the evaluation, the color image Lena is contaminated with 4% *salt and pepper* noise.

Method	NMSE [10^{-4}]	RMSE	PSNR [dB]
None	514.95	32.165	17.983
AMF	82.863	12.903	25.917
VMF	23.304	6.842	31.427
ANNF	31.271	7.926	30.149
BVDF	29.074	7.643	30.466
HDF	22.845	6.775	31.513
AHDF	22.603	6.739	31.559
DDF	24.003	6.944	31.288
FVDF	26.755	7.331	30.827
Proposed			
$\mu_1(x)$	4.959	3.157	38.145
$\mu_2(x)$	5.398	3.294	37.776
$\mu_3(x)$	9.574	4.387	35.288
$\mu_4(x)$	5.064	3.190	38.054
$\mu_5(x)$	4.777	3.099	38.307
$\mu_6(x)$	11.024	4.707	34.675
$\mu_7(x)$	4.693	3.072	38.384

TABLE 3.4 Comparison of the new filter results (RMSE) using different vector norms (Lena contaminated with 4% *salt and pepper* noise).

Filters	L_1	L_2	L_3	L_∞
$\beta_1(x)$	3.615	3.157	3.172	3.462
$\beta_5(x)$	3.579	3.099	3.167	3.694
$\beta_7(x)$	3.838	3.072	3.138	3.752

shows the results of image filtering using the new method in comparison with the VMF. For the comparison color test image Lena was used and the image pixels were distorted by 4% *salt and pepper* impulsive noise. Figure 3.4 depicts the efficiency of the new filter in comparison with the VMF, BVDF, and DDF for different percentages of impulsive noise.

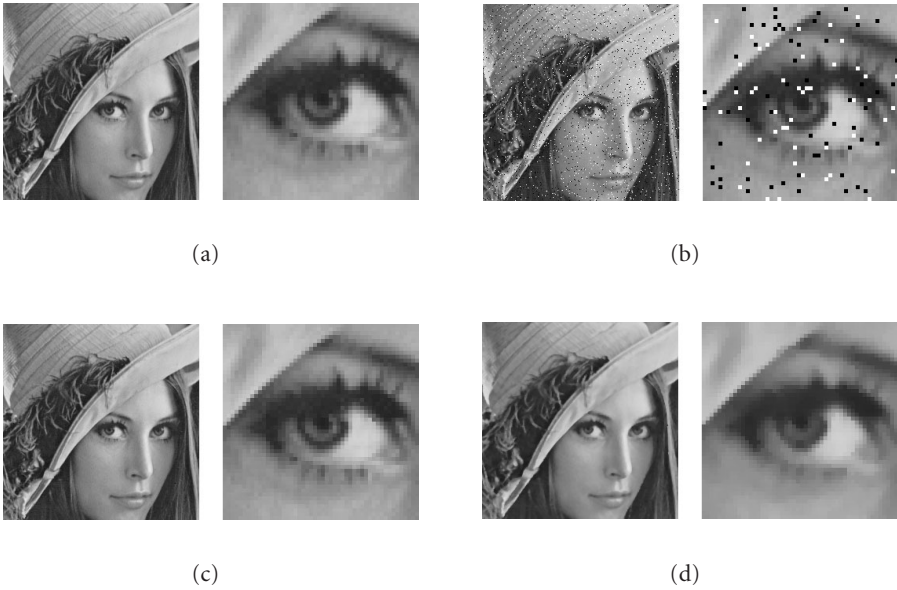


FIGURE 3.2 Noise-reduction effect of the proposed filter as compared with the standard median filter: (a) gray-scale test image Lena, (b) image distorted by 4% salt and pepper noise, (c) image filtered with the new method $\beta_1 = 5.04 \times 10^{-3}$ (PSNR = 42.02), (d) median filter (PSNR = 34.08). To the right are the zoomed image portions.

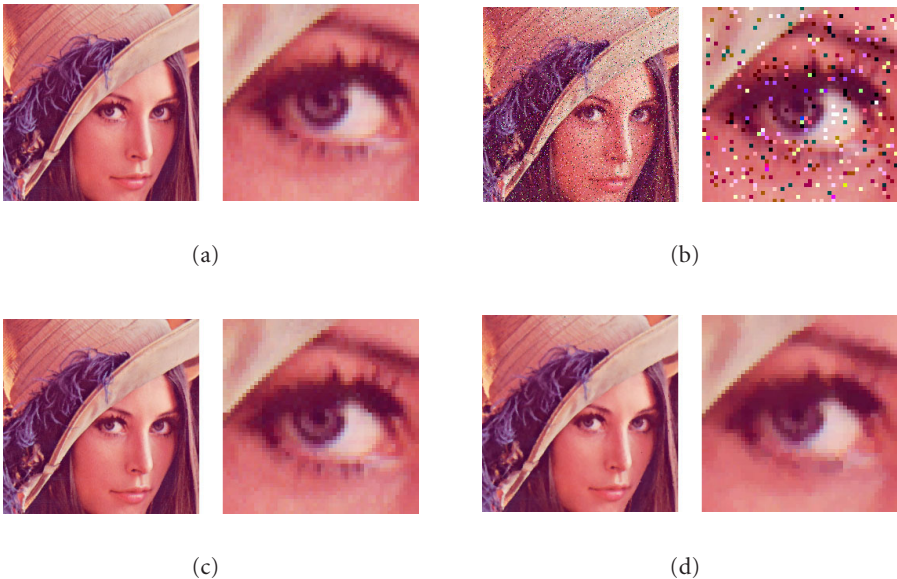


FIGURE 3.3 Noise-reduction effect of the proposed filter as compared with the vector median filter: (a) color test image Lena, (b) image distorted by 4% impulsive noise, (c) new method $\beta_1 = 5.04 \times 10^{-3}$ (PSNR = 38.15), (d) VMF (PSNR = 31.43). To the right are the zoomed image portions.

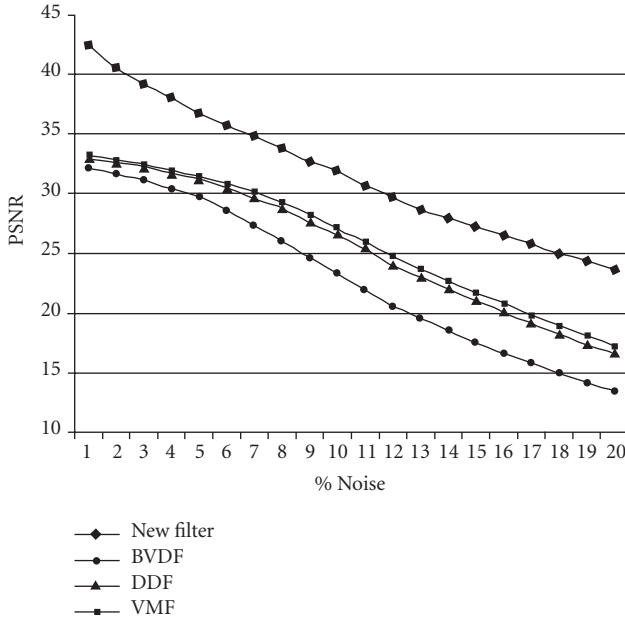


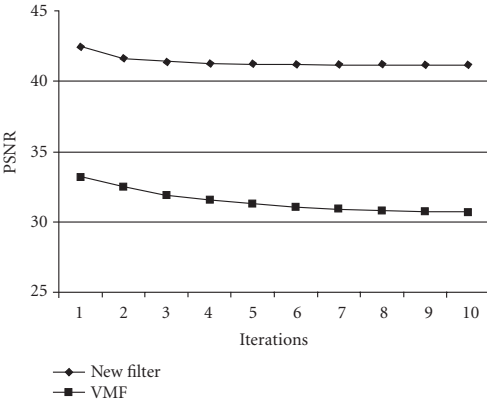
FIGURE 3.4 Dependence of the noise reduction efficiency on the percentage of impulsive noise for the new method, VMF, BVDF, and DDF (Lena color image, $\beta_1 = 5.04 \times 10^{-3}$).

As can be seen, the new class of filters eliminates efficiently impulsive noise, while preserving important image structures like edges, corners, lines, and fine texture (Figures 3.2 and 3.3). Another interesting property of the presented method of noise attenuation is shown in Figures 3.5 and 3.6. After a relatively small number of iterations, the filter converges to the root signal, meaning that in further iterations no changes are introduced to the image.

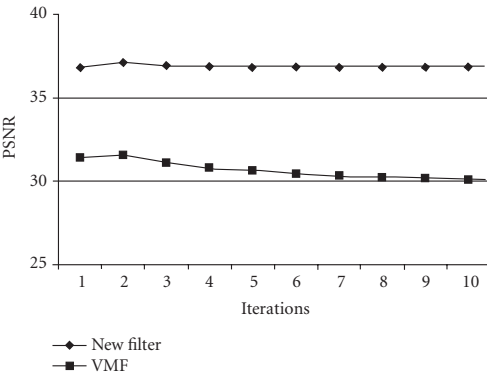
According to the results presented in this section, the best performance is achieved when a similarity function is inversely proportional to the distance between the vector signals (μ_7). Although someone can argue that the shape and the parameters of the “optimal” similarity function are application-dependent, determined mainly by the nature of the image and the type of noise corruption, we claim that the functions introduced here are easy to build and implement, require minimum user intervention in terms of parameter tuning, provide acceptable results for a wide range of input images, and are robust to suboptimal β_i parameters.

4. Conclusions

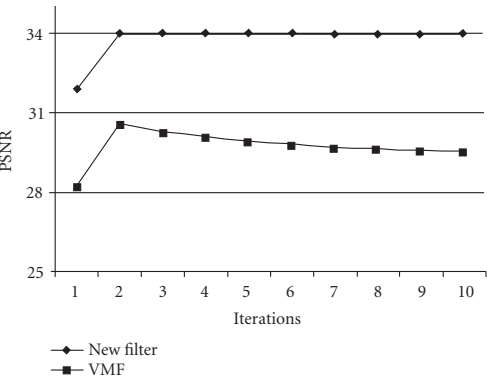
In this paper, a new class of filters has been presented. Experimental results indicate that the new method of noise reduction significantly outperforms standard procedures used to restore gray scale and color images contaminated with impulsive noise. The new technique is fast and very easy to implement. The BASIC code is given in Algorithm 2.1 so that the filter can be easily evaluated by the image processing community.



(a)



(b)



(c)

FIGURE 3.5 Dependence of the noise reduction efficiency of the proposed filter and VMF on the number of iterations for color test images distorted by (a) 1% impulsive noise, (b) 5% impulsive noise, (c) 10% impulsive noise. (Lena color image, $\beta_1 = 5.04 \times 10^{-3}$).

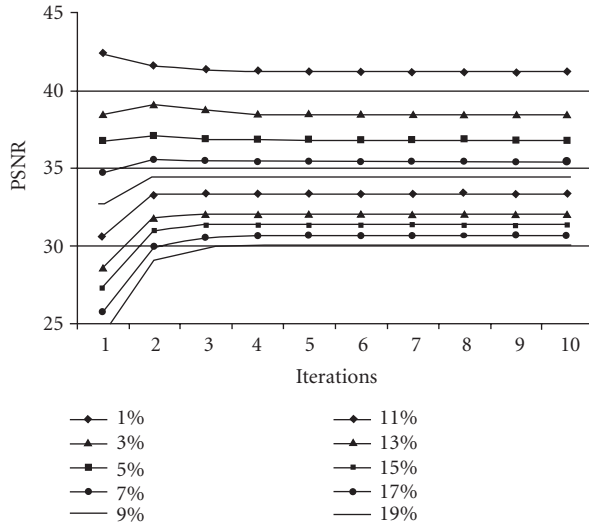


FIGURE 3.6 Dependence of the noise reduction efficiency of the new filter on the number of iterations for different percentages of impulsive noise (Lena color image, $\beta_1 = 5.04 \times 10^{-3}$).

Acknowledgment

B. Smolka is supported by the KBN Grant 4T11F01824.

References

- [1] J. Astola, P. Haavisto, and Y. Neuovo, *Vector median filters*, Proc. IEEE **78** (1990), no. 4, 678–689.
- [2] M. Gabbouj and F. A. Cheikh, *Vector median-vector directional hybrid filter for color image restoration*, Proceedings of European Signal Processing Conference (Trieste, 1996), vol. 2, EURASIP, Switzerland, 1996, pp. 879–882.
- [3] D. G. Karakos and P. E. Trahanias, *Generalized multichannel image-filtering structures*, IEEE Trans. Image Process. **6** (1997), no. 7, 1038–1045.
- [4] R. Lukac, *Color image filtering by vector directional order-statistics*, Pattern Recognition and Image Analysis **12** (2002), no. 3, 279–285.
- [5] ———, *Optimised directional distance filter*, Machine Graphics and Visions **11** (2002), no. 2-3, 311–326.
- [6] ———, *Adaptive vector median filtering*, Pattern Recognition Lett. **24** (2003), no. 12, 1889–1899.
- [7] I. Pitas and P. Tsakalides, *Multivariate ordering in color image filtering*, IEEE Trans. Circuits and Systems for Video Technology **1** (1991), no. 3, 247–259.
- [8] I. Pitas and A. N. Venetsanopoulos, *Nonlinear Digital Filters: Principles and Applications*, Kluwer Academic Publishers, Massachusetts, 1990.
- [9] ———, *Order statistics in digital image processing*, Proc. IEEE **80** (1992), no. 12, 1893–1921.
- [10] K. N. Plataniotis, D. Androustos, and A. N. Venetsanopoulos, *Color image processing using adaptive vector directional filters*, IEEE Trans. on Circuits and Systems II: Analog and Digital Signal Processing **45** (1998), no. 10, 1414–1419.
- [11] K. N. Plataniotis and A. N. Venetsanopoulos, *Color Image Processing and Applications*, Springer-Verlag, Berlin, 2000.

- [12] B. Smolka, K. N. Plataniotis, A. Chydzinski, A. N. Venetsanopoulos, and K. W. Wojciechowski, *On the reduction of impulsive noise in multichannel image processing*, *Optical Engineering* **40** (2001), no. 6, 902–908.
- [13] B. Smolka and K. Wojciechowski, *Random walk approach to image enhancement*, *Signal Process.* **81** (2001), no. 3, 465–482.
- [14] P. E. Trahanias and A. N. Venetsanopoulos, *Vector directional filters—a new class of multichannel image processing filters*, *IEEE Trans. Image Process.* **2** (1993), no. 4, 528–534.

B. Smolka: Department of Automatic Control, Electronics and Computer Science, Silesian University of Technology, 16 Akademicka Street, 44-101 Gliwice, Poland

E-mail address: bsmolka@ia.polsl.gliwice.pl

A. Chydzinski: Department of Automatic Control, Electronics and Computer Science, Silesian University of Technology, 16 Akademicka Street, 44-101 Gliwice, Poland

E-mail address: andyndy@polsl.gliwice.pl

K. N. Plataniotis: Edward S. Rogers Sr. Department of Electrical and Computer Engineering, University of Toronto, 10 King's College Road, Toronto, Ontario, Canada M5S 3G4

E-mail address: kostas@dsp.toronto.edu

A. N. Venetsanopoulos: Edward S. Rogers Sr. Department of Electrical and Computer Engineering, University of Toronto, 10 King's College Road, Toronto, Ontario, Canada M5S 3G4

E-mail address: anv@dsp.toronto.edu